

## Supporting Information:

### Water-solubilized, Cap-Stabilized, Helical Polyalanines: Calibration Standards for NMR and CD Analyses

Gabriel E. Job, Bjoern Heitmann, Robert J. Kennedy, Sharon M. Walker, and Daniel S. Kemp

#### Calculational Appendix.

**A. Equivalence of eqs. (1) = (9) and (10`).** By defining the required length standards  $[\theta]_{\lambda,n}$ , eq. (1) underlies all quantitative calculations of FH from peptide CD residue ellipticities. Eq. (1) is justified by theory and by least squares deconvolution of CD spectra of proteins with known secondary structures. This Section introduces a core length  $(n - k)$  as an explicit term in ellipticity modeling and demonstrates that the molar ellipticity as expressed in eq. (10`) is fully equivalent to eqs. (1) and (9). [Eq. (9) is a molar ellipticity equivalent of eq. (1), obtained by multiplication by  $n$ .]

Eq. (10) rests on the assumption that for a particular length series of completely helical homopeptides the molar ellipticity of any peptide of sufficient length can be approximated accurately as a sum of two terms, a core ellipticity that depends on the overall helical length of the peptide but not on the structure of its N- and C-terminal caps, and a capping ellipticity that is dependent on cap structure but is independent of peptide length. Eq. (11) equates this core ellipticity with a product of a residue ellipticity  $[\theta]_{\lambda,\infty}$  and a core length,  $(n - k)$ ; this equation rests on the assumption, justified by theory, that for homopeptides of sufficient length, central regions of length  $(n - k)$  exist with the property that if the length of any peptide is extended by one residue, its molar ellipticity increases by the length and cap-independent parameter  $[\theta]_{\lambda,\infty}$ , which depends only on the physical conditions of the experiment and (possibly) the nature of the homopeptide residue. The length parameter  $k$  is defined such that all peptides of length greater than  $k$  meet the above conditions. Peptides of length less than or equal to  $k$  then must lack a convergent core region with these properties.

$$[\theta]_{\lambda,n} = [\theta]_{\lambda,\infty} (1 - X/n) \quad (1)$$

$$[\theta_{\text{Molar}}]_{\lambda,n} = [\theta]_{\lambda,\infty} (n - X) = [\theta]_{\lambda,\infty} n - [\theta]_{\lambda,\infty} X = [\theta]_{\lambda,\infty} (n - k) - [\theta]_{\lambda,\infty} (X - k) \quad (9)$$

$$[\theta_{\text{Molar}}]_{\lambda,n} = [\theta_{\text{Molar}}]_{\lambda,\text{Core},n} + [\theta_{\text{Molar}}]_{\lambda,\text{Caps}} \quad (10)$$

$$[\theta_{\text{Molar}}]_{\lambda,\text{Core},n} = [\theta]_{\lambda,\infty} (n - k) \quad (11)$$

$$[\theta_{\text{Molar}}]_{\lambda,n} = [\theta]_{\lambda,\infty} (n - k) + [\theta_{\text{Molar}}]_{\lambda,\text{Caps}} \quad (10')$$

$$X \equiv k - [\theta_{\text{Molar}}]_{\lambda,\text{Caps}} / [\theta]_{\lambda,\infty} \quad (12)$$

$$[\theta_{\text{Molar}}]_{\lambda,\text{Caps}} = [\theta]_{\lambda,\infty} (k - X) \quad (12')$$

Peptide CD chromophores are characterized by electronic transitions involving a series of  $\phi$  and  $\psi$ -oriented pairs of amides that flank residue  $\alpha$ -carbons; near the peptide ends

the chromophores are expected to have anomalous properties that reflect the presence of capping functions. The value of  $k$  is defined in part by the length of this anomalous region. Since N- and C-terminal  $\alpha$ -helical loops contain 3 residues that lack a full complement of intrahelical contacts, the minimum value of  $k$  for a simple N- and C-capped peptide is probably six. This is a lower bound, since the intensity of the helical CD chromophore of a peptide residue depends upon helix length.

It is convenient to scale the molar ellipticity  $[\theta_{\text{Molar}}]_{\lambda, \text{Caps}}$  contributed by the capping region as a length by dividing it by the limiting residue ellipticity  $[\theta]_{\lambda, \infty}$ . The difference between this scaled length and  $k$  defines the length parameter  $X$  of eqs. (1) and (9), as seen in eq. (12). The value of  $[\theta_{\text{Molar}}]_{\lambda, \text{Caps}}$  can equivalently be expressed as a function of  $X$  as in eq.(12'). Substitution of eq. (12') into eq. (10'), cancellation of  $k$  terms, and division by  $n$  yields eq. (1). Substitution of eq.(12) into the right hand form of eq. (9) yields eq. (10'), as expected from the definition of  $X$ .

### **B. Steps in assignment of $[\theta]_{\lambda, \infty}$ and $X$ from a proposed $\text{Ala}_n$ calibration series.**

1. Two types of core convergence must be demonstrated by CD-independent methods. First, spectroscopic properties that reflect variations in local structure must be constant for core residue candidates. Second, a property that reflects helical energetics must be limiting and length-independent for core residues. These conditions provide a candidate value for the non-core length  $k$ .

2. The fractional helicities  $\text{FH}$  of all members of the calibration series must be assigned, and site helicities  $\text{FH}_i$  for all residues in the core regions identified in 1. must closely approximate 1.0. Two points are key. First, if  $\text{FH}_i < 1.0$  and varies with overall length  $n$  for core residues, the homopeptides do not comprise a calibration series, since the slope of the linear length regression, even if defined with precision, cannot be interpreted as equal to a limiting residue ellipticity  $[\theta]_{\lambda, \infty}$ . Second, for assignment of  $[\theta]_{\lambda, \infty}$  it is not essential that the  $k$  residues of the capping regions have limiting  $\text{FH}_i$ , ***provided those values are defined, are site-specific, and can be shown for each calibration series member to be independent of the overall peptide length  $n$ .***

3. Since the intensities of molar ellipticities for a peptide length series are expected to correlate strongly with length, a high percentage of the members of the calibration series must exhibit molar ellipticity values that significantly exceed the value for the shortest series member. This property ensures that the core term of eq. (10) dominates the cap term for most members of the calibration series.

4. A high quality linear regression must be demonstrable at all wavelengths if experimental molar ellipticities for series members are correlated with length. Slopes must remain constant, within experimental error, if shorter members of the series are excluded from the regression. The quality of this regression tests the validity of eqs. (1), (9), and (10'). If the test is passed, it also assigns  $[\theta]_{\lambda, \infty}$  as a series of regression slopes.

5. Two further tests can be used to validate the remaining assumption that  $[\theta_{\text{Molar}}]_{\lambda, \text{Caps}}$  is length-independent. First, the value of  $[\theta_{\text{Molar}}]_{\lambda, \text{Caps}}$  that can be extrapolated from the regression by setting  $n = k$ , should, within measurement error, equal the experimental value measured  $[\theta_{\text{Molar}}]_{\lambda, k}$ . Second, in a wavelength region in which  $[\theta]_{\lambda, \infty}$  changes sign and at the  $\lambda$  value at which  $[\theta]_{\lambda, \infty} = 0$ , equation (10') reduces to  $[\theta_{\text{Molar}}]_{\lambda, n} = [\theta_{\text{Molar}}]_{\lambda, \text{Caps}}$ , implying that the values of are length-independent. Within measurement error, this length independence must be demonstrable for the members of the calibration series at this wavelength.

6. If the above tests are met, as discussed in the text, a value of X can be assigned if the linear length regression is carried out using values of  $[\theta_{\text{Molar}}]_{\lambda,n}$  have been corrected by subtracting a capping value  $[\theta_{\text{Molar}}]_{\lambda,0}$  and dividing the difference by  $\text{FH}_n$  values.

**C. Problems associated with X assignments.** The above derivations make clear that the parameter  $[\theta]_{\lambda,\infty}$  reflects the length dependencies of molar ellipticities for members of a calibrating peptide series as n is increased to large values. The parameter X primarily reflects properties that dominate very short series members, characterized by modest values of  $[\theta_{\text{Molar}}]_{\lambda,n}$ . Moreover, unlike  $[\theta]_{\lambda,\infty}$ , which for a homopeptide is a function solely of the measurement conditions and the nature of the amino acid residue, the value of X is likely to be sensitive to local structural features of the first and last helical loops within the peptide sequence. X may also be wavelength-dependent. Theory implies that different length dependences are characteristic of the  $\pi-\pi^*$  and  $n-\pi^*$  transitions that underlie helical chiroptic phenomena, and these should be reflected in a significant  $\lambda$ -dependence for X. All these considerations imply that for maximum precision, X must be tailored to the structures of the end caps that appear in a peptide series of current interest.

In the present study, values of both  $[\theta]_{\lambda,\infty}$  and X were assigned from a data base of  $[\theta_{\text{Molar}}]_{\lambda,n}$  values measured for a large length range of N- and C-capped peptides by subtracting a  $[\theta_{\text{Molar}}]_{\lambda,0}$  correction for the portion of each  $[\theta_{\text{Molar}}]_{\lambda,n}$  that is contributed by the Trp UV reporter, solubilizers, spacers, and the helix-stabilizing caps  $^{\beta}\text{Asp-Hel}$  and *beta*. A fundamental uncertainty that accompanies this use of cap-corrected  $[\theta_{\text{Molar}}]_{\lambda,n}$  values arises from the likelihood that conformations and thus ellipticity contributions in the  $^{\beta}\text{Asp-Hel}$  and *beta* region of the correction peptide are atypical of normal series members in which these functions flank an  $\text{Ala}_n$  core. A lower bound for this uncertainty is provided by comparing pairs of cap-corrected  $[\theta_{\text{Molar}}]_{\lambda,n}$  values for peptides of identical length taken from series 2 and series 3. The error in measurement for each series is estimated as 3 to 5%, implying an error in the comparison that lies in the range of 6 to 10%. The actual average percentage differences calculated over the range of 208 to 228 nm is 5% for  $n = 14$  or 16; 11% for  $n = 12$ , and 15% for  $n = 10$ . These provide estimates for a lower bound to cap correction errors. As noted in the text, these uncertainties are likely to result in accuracy errors that are much larger for X than for  $[\theta]_{\lambda,\infty}$ , which is primarily sensitive to the ellipticities of the longer series members.

**D. Calculation of  $\text{FH}_i$  and FH Values from  $\text{PF}_i$ -Derived  $\text{FH}_{\text{NH}_i}$  Values.** The purpose of this section is to provide a verification of the inequalities of eqs. (5), (6), & (7) used in the text to calculate values of  $\text{FH}_i$  from  $\text{PF}_i$ -derived values of  $\text{FH}_{\text{NH}_i}$ . Relationships between these different measures of site helicity have been reported,<sup>8</sup> but this section focuses on the semi-quantitative relationships that result for  $\text{PF}_i$  values of 20 to 200, corresponding to  $\text{FH}_{\text{NH}_i}$  values that exceed 0.95. Inspection of Fig. 1c shows that within the body of an  $\alpha$ -helix, a helical hydrogen bond between the carbonyl oxygen of the  $(i - 4)^{\text{th}}$  residue and the NH of the  $i^{\text{th}}$  residue can form only if each of the  $\phi$ ,  $\psi$  dihedral angle pairs at residues  $(i - 1)$ ,  $(i - 2)$ , and  $(i - 3)$  are helical. Since  $\text{FH}_i$  is defined as the site helicity at the  $i^{\text{th}}$   $\alpha$ -carbon,  $\text{FH}_{\text{NH}_i} = 1.0$  implies that  $\text{FH}_{i-1} = \text{FH}_{i-2} = \text{FH}_{i-3} = 1.0$ . The analysis of Table II (below) generalizes this relationship by examining the possible conformational states that can influence values of  $\text{FH}_{\text{NH}_i}$ ,  $\text{FH}_{i-1}$ ,  $\text{FH}_{i-2}$ , and  $\text{FH}_{i-3}$  within any four-residue helical sequence. In the Lifson-Roig (h = helix, c = coil) formalism, the  $2^n$  conformations of an N- and C-capped peptide of n residues can be grouped within

seven local sequences.<sup>1</sup> Thus a partial sequence hhh symbolizes the collection of all helical conformations that include  $\alpha$ -carbons at residues (i - 1), (i - 2), and (i - 3); ccc includes conformations that are nonhelical within these residues. Similarly, hcc and hhc respectively correspond to helical sequences that terminate at either residue (i - 3) or (i - 2), and cch and chh correspond to helical sequences that are initiated at either residue (i - 2) or (i - 1). Sequence hch corresponds to a pair of collective helical conformations, one terminated at residue (i - 3), the other initiated at residue (i - 1).

Identifiers, mole fractions, and the contribution to  $FH_{\text{NH}_i}$  by each of these appear in the first three columns of Table II. The h symbols that appear in the three vertical columns identify mole fractions that comprise  $FH_{i-1}$ ,  $FH_{i-2}$ , and  $FH_{i-3}$ . Thus, by reading down the first column of the Table,  $FH_{i-3}$  is found by adding all mole fractions corresponding to a helical  $\alpha$ -carbon at this site:  $FH_{i-3} = (\chi_{\text{hhh}} + \chi_{\text{hhc}} + \chi_{\text{hcc}} + \chi_{\text{hch}})$ . Similarly,  $FH_{i-2} = (\chi_{\text{hhh}} + \chi_{\text{hhc}} + \chi_{\text{chh}})$ , and  $FH_{i-1} = (\chi_{\text{hhh}} + \chi_{\text{cch}} + \chi_{\text{chh}} + \chi_{\text{hch}})$ . Adding these and dividing by 3 yields  $(FH_{i-1} + FH_{i-2} + FH_{i-3})/3 = \chi_{\text{hhh}} + 2(\chi_{\text{hhc}} + \chi_{\text{chh}} + \chi_{\text{hch}})/3 + (\chi_{\text{hcc}} + \chi_{\text{cch}})/3$ . From the fifth column, one sees that  $\chi_{\text{hhh}} = FH_{\text{NH}_i}$ , which proves the inequality of eq. (5): the mean of the three  $FH_i$  at sites that precede i must be greater than the value of  $FH_{\text{NH}_i}$ . As noted previously, the presence of central peptide regions in which values of  $FH_{\text{NH}_i}$  remain constant and exceed 0.99 implies that the helical manifold is dominated by the fully helical conformation, with a minor contribution from the nonhelical conformation. In these regions,  $FH_i$  and  $FH_{\text{NH}_i}$  are in good agreement.

For the last residues of peptides of series 2 or series 3, the values of  $FH_{\text{NH}_i}$  decrease monotonically with increasing i. This C-terminal fraying effect can be readily interpreted as due to a change in the relative magnitudes of the mole fractions of Table II. Helical conformations corresponding to part structures hhh, hhc, or hcc contribute significantly, but conformations corresponding to part structures cch, chh, or hch do not, since these initiate exceptionally short helical sequences. Inspection shows that for a Table comprised only of hhh, hhc, hcc, and ccc conformations,  $FH_{\text{NH}_i} = FH_{i-1}$ , and  $FH_{i-3} > FH_{i-2} > FH_{i-1}$ , and the value of  $FH_{\text{NH}_i}$  is to a good approximation modeled by eq. (7). From a similar argument, eq. (6) models  $FH_{\text{NH}_i}$  for  $i \ll n$ . For the two cases in which either  $i = 4$ , or  $i = n + 1$ , this argument implies that, as noted previously,<sup>8</sup> the values of  $FH_i$  can be rigorously defined as  $FH_{\text{NH}_4} = FH_1$  for the former (for which  $\chi_{\text{hhc}}$ ,  $\chi_{\text{hcc}}$ , and  $\chi_{\text{hch}}$  are all zero) and  $FH_{\text{NH}(i+1)} = FH_n$  for the latter (for which  $\chi_{\text{cch}}$ ,  $\chi_{\text{chh}}$ , and  $\chi_{\text{hch}}$  are all zero).

**Table II** Grouped Conformational States at Three Peptide  $\alpha$ -Carbons that Precede a Site i

Peptide Site:	(i - 3)	(i - 2)	(i - 1)	Mole Fraction	Contributes to $FH_{\text{NH}_i}$ ?
	h	h	h	$\chi_{\text{hhh}}$	yes
	h	h	c	$\chi_{\text{hhc}}$	no
	h	c	c	$\chi_{\text{hcc}}$	no
	c	c	h	$\chi_{\text{cch}}$	no
	c	h	h	$\chi_{\text{chh}}$	no
	h	c	h	$\chi_{\text{hch}}$	no
	c	c	c	$\chi_{\text{ccc}}$	no

(1) In the Lifson-Roig formalism, helical  $\phi$ ,  $\psi$  angles at isolated single residues (chc) or pairs of residues (chhc) do not contribute to the helical state sum. As a result, in the context of Table II, the symbolism ccc is an abbreviation for all global conformations that contain the following local sequences: |ccc|, |chc|, |chcc|, |chhc|, |cchc|, |chhc|.

To provide a quantitative confirmation of these qualitative arguments, eqs. (6) and (7) were validated by a series of Lifson-Roig calculation of values for  $FH_i$ , and  $FH_{NH_i}$ . Length-dependent  $w$  values assigned for a spaced, solubilized  $Ala_n$  series were employed<sup>52</sup> as well as an N-capping parameter of 200 for  $^{\beta}AspHel$ ,  $pH > 4.5$ , and a C-capping parameter of 6 for *beta*. For values of  $FH_{NH_i}$  that fall above 0.95 but below 0.99 and  $Ala_n$  lengths  $n = 24, 14, \text{ and } 10$ , respective fit deviations of 0.2, 0.5, and 0.8 % were calculated.

#### E. Extrapolation of Assigned FH Values for Series 2, Table I of text

Consistent with the treatment of  $[\theta_{Molar}]$  values as sums of cap and core contributions, eq. (13) uses data of Figure 10 to calculate extrapolated lower limits for the overall FH as a sum of contributions of a core region of length  $(n - 6)$  with a constant  $FH_{core,low}$  value, and six length-independent lower limits for site helicities at the indicated sites. Eq. (14) defines the analogous upper limits.

$$FH_{Ext,low} = (FH_{1,low} + (n - 6)FH_{core,low} + FH_{(n-4),low} + FH_{(n-3),low} + 2 FH_{(n-2),low} + 0.1)/n \quad (13)$$

$$FH_{Ext,high} = (FH_{1,high} + (n - 6)FH_{core,high} + FH_{(n-4),high} + FH_{(n-3),high} + 2 FH_{(n-2),high} + 0.7)/n \quad (14)$$

#### F. NMR Data

Table I <sup>1</sup>H Chemical Shift Assignments for the Peptide Ac- $^{\beta}$ AspHel- $Ala_8$ -*beta*-NH<sub>2</sub> in D<sub>2</sub>O  
2 °C (ppm)

(DSS was used as an internal reference)

Ac: 2.027;

$^{\beta}Asp$ : HN, 8.623; HA, 4.813; HB2, 3.267; HB3, 2.735;

Hel: H2, 4.704; H13a, 2.531; H13b, 3.007; H11, 3.888; H12b, 4.199; H12a, 4.118; H5, 4.69; H6a, 2.299; H6b, 2.476; H7a, 2.071; H7b, 1.993; H8, 4.654; H9a, 3.198; H9b, 2.862

A1: HN, 7.393; HA, 4.292; HB, 1.441; A2: HN, 8.222; HA, 4.189; HB, 1.451;

A3: HN, 8.279; HA, 4.2; HB, 1.469; A4: HN, 7.974; HA, 4.211; HB, 1.48;

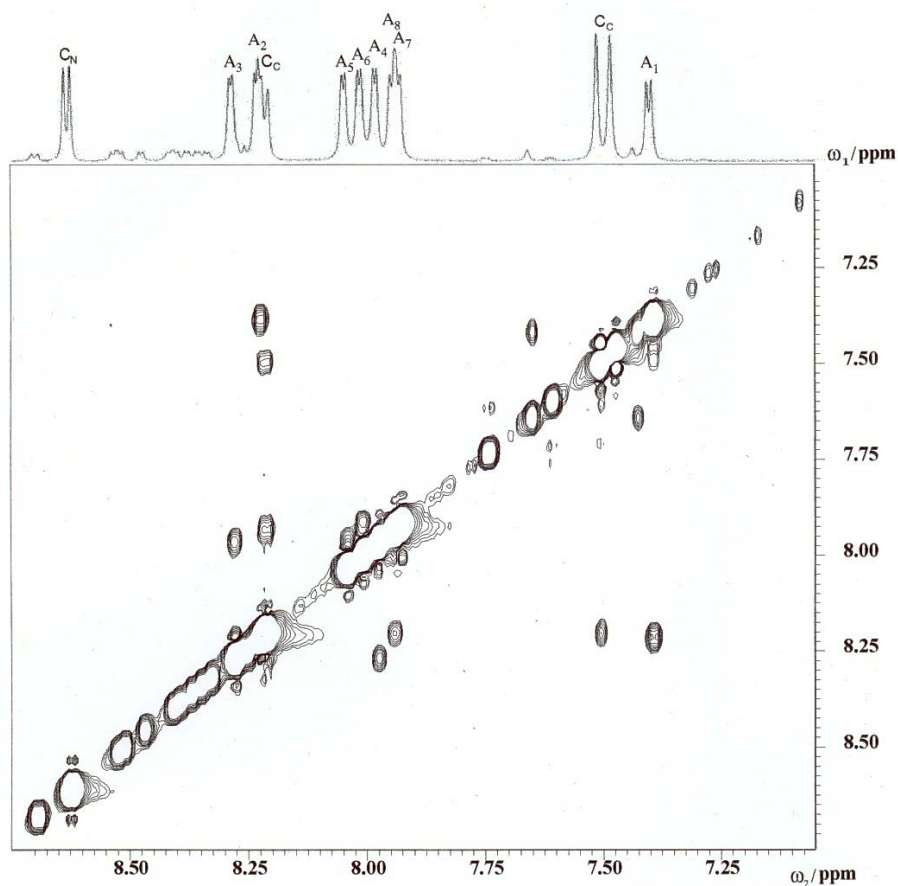
A5: HN, 8.039; HA, 4.223; HB, 1.469; A6: HN, 8.007; HA, 4.181; HB, 1.469;

A7: HN, 7.925; HA, 4.211; HB, 1.469; A8: HN, 7.941; HA, 4.3; HB, 1.469;

*beta*: HN, 8.212; HA, 4.721; HB2, 3.559; HB3, 3.357; HN2, 7.996;

NH<sub>2</sub>: HN1, 7.506; HN2, 7.474

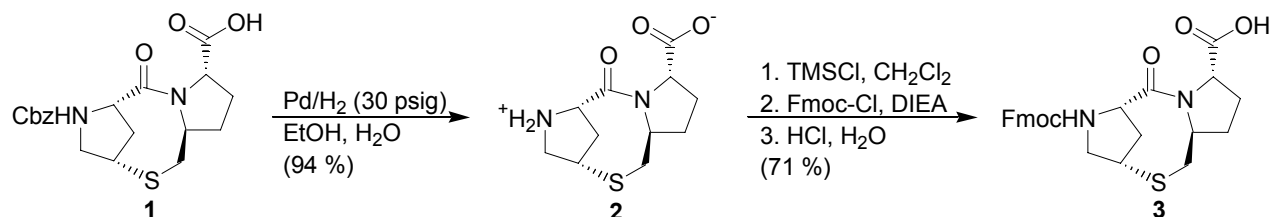
ROESY Spectrum (ppm) for the peptide  $\text{Ac-}\beta\text{-AspHel-Ala}_8\text{-beta-NH}_2$  in  $\text{H}_2\text{O/D}_2\text{O}$  (95/5, v/v) 40 mM phosphate buffer, 2 °C, pH 4.5 (DSS was used as an internal reference)



## I. Synthesis

### Fmoc-Amino Acid Synthesis

The published synthesis<sup>2</sup> of the *N*-protected helical template, Fmoc-Hel-OH, was modified as shown in the scheme below.



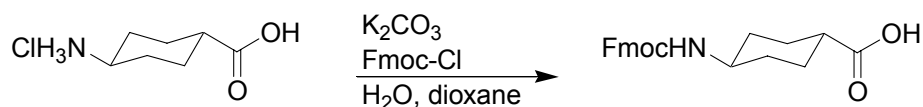
**2-Oxo-9-thia-3,12-diaza-tricyclo[8.2.1.0<sup>3,7</sup>]tridecane-4-carboxylic acid, 2**

<sup>2</sup> Maison, W.; Arce, E.; Renold, P.; Kennedy, R. J.; Kemp, D. S. *J. Am. Chem. Soc.* **2001**, *123*, 10245.

The acid **1** (1.0 g, 2.6 mmol) was taken up in 60 mL ethanol and transferred to a Parr bottle containing 4.0 g of Pd/C (10 %, 50% weight H<sub>2</sub>O). The vessel was then placed in a Parr shaker and H<sub>2</sub> was applied at 30 psig. After 24 h the reaction was stopped and the mixture was filtered to remove the catalyst; solvent was removed in vacuo to yield 0.47 g (72%) of the title compound as a light yellow foam. <sup>1</sup>H NMR (CDCl<sub>3</sub>, 300 MHz) δ 8.19 (broad s, 2H), 5.35 (broad s, 1H), 4.53 (dd, 1H, J = 7.1, 3.0 Hz), 4.28 (d, 1H, J = 10.4 Hz), 3.54 (m, 2H), 3.37 (d, 1H, J = 9.5 Hz), 2.84 (dd, 1H, J = 15.9, 6.6 Hz), 2.67 (m, 2H), 2.28 (m, 2H), 2.06 (m, 2H), 1.78 (d, 1H, J = 10.2). <sup>13</sup>C NMR (CDCl<sub>3</sub>, 125 MHz): δ 175.3, 172.3, 62.1, 61.9, 58.9, 55.1, 40.8, 38.8, 38.0, 34.2, 25.8. HRMS calcd for [C<sub>11</sub>H<sub>16</sub>N<sub>2</sub>O<sub>3</sub>S + H] 257.0954, found 257.0963. IR (cm<sup>-1</sup>): 1172, 1408, 1588, 1710, 2954, 3364. IR (cm<sup>-1</sup>): 1172, 1408, 1588, 1710, 2954, 3364; [α]<sub>D</sub><sup>23</sup> = +48.6 (c 1.20, CHCl<sub>3</sub>).

*2-Oxo-9-thia-3,12-diaza-tricyclo[8.2.1.0<sup>3,7</sup>]tridecane-12-fluorenylmethoxycarbonyl-4-carboxylic acid, 3*

The procedure of Bolin et al.<sup>3</sup> was used to add the Fmoc group to **2**. The amino acid **2** (0.47g, 1.9 mmol) and TMS-Cl (0.47 mL, 3.7 mmol) were heated at reflux in 40 mL of CH<sub>2</sub>Cl<sub>2</sub> for 1 h. The solution was then cooled with an ice bath and DIEA (0.59 mL, 3.4 mmol) was added, followed by Fmoc-Cl (0.49g, 1.9 mmol). The solution was allowed to warm to room temperature for 1.5 h. The contents of the reaction vessel were concentrated in vacuo to yield a light yellow oil. A solution of NaHCO<sub>3</sub> (25 mL, 2.5%) and diethyl ether (25 mL) were added, and the mixture was stirred vigorously until the oil had been partitioned between the two layers. The aqueous layer was washed with diethyl ether (1 x 25 mL); the combined organic layers were washed with a 2.5% bicarbonate solution (2 x 25 mL). The combined aqueous layers were acidified, with cooling, to pH 2 with a 6 M solution of HCl. A solid formed and was extracted with CH<sub>2</sub>Cl<sub>2</sub> (3 x 50 mL). The solution of methylene chloride was dried over MgSO<sub>4</sub> and filtered. The solvent was removed in vacuo to yield 0.65 g (71 %) of the title compound as a pale yellow foam. The <sup>1</sup>H NMR and <sup>13</sup>C NMR of this product were identical to those of an authentic sample of **3** obtained by the original method<sup>2</sup>.



*trans-4-(Fluorenylmethoxycarbonylamino)-cyclohexanecarboxylic acid*

To a cold solution of 1 M K<sub>2</sub>CO<sub>3</sub> (26 mL) and dioxane (10 mL) was added *trans*-4-aminocyclohexanecarboxylic acid hydrochloride (1.0 g, 5.6 mmol). Fmoc-Cl (1.45 g, 5.6 mmol) was added to the reaction and the mixture was stirred at 0 °C for 5h and then allowed to warm to room temperature overnight. The milky reaction mixture was then poured into 300 mL of

<sup>3</sup> Bolin, D. R.; Sytwu, I.-I.; Humiec, F.; Meienhofer, J. *Int. J. Peptide Protein Res.* **1989**, *33*, 353.

water; with some shaking all solids went into solution. The aqueous mixture was extracted with diethyl ether (2 x 100 mL). The organic extracts were discarded and the aqueous solution was cooled on an ice bath. The aqueous layer was acidified to pH 2 with 6 M HCl; the solid that formed was collected by vacuum filtration and washed well with water. The filter cake was air-dried overnight and then dried under vacuum. This crude product was found to be sufficiently pure to use in the synthesis of peptides. A small sample was recrystallized from acetonitrile and fully characterized. <sup>1</sup>H NMR (d<sub>6</sub>-DMSO, 500 MHz), major amide rotamer: δ 12.02 (s, 1H), 7.89 (2H, d, J = 7.6 Hz), 7.68 (2H, d, J = 7.5 Hz), 7.41 (2H, t, J = 7.3 Hz), 7.33 (2H, t, J = 7.5 Hz), 7.24 (1H, d, J = 7.5 Hz), 4.27 (2H, d, J = 6.9 Hz), 4.20 (1H, t, J = 6.3 Hz), 3.22 (1H, m), 2.09 (1H, t, J = 11.8 Hz), 1.88 (2H, d, J = 12.1 Hz), 1.81 (2H, d, 10.4 Hz), 1.33 (2H, quart, J = 11.9 Hz), 1.18 (2H, quart, J = 11.1 Hz). Signals arising from the minor amide rotamer are visible; all of these signals are broad and poorly resolved: δ 7.63, 6.68, 4.44, 1.96, 1.75, 1.46, 1.10, 0.94. The minor peaks merge with those of the major rotamer at 60 °C. <sup>13</sup>C (d<sub>6</sub>-DMSO, 125 MHz): δ 176.48, 155.35, 143.96, 140.76, 127.62, 127.07, 125.21, 120.15, 65.12, 49.14, 46.78, 41.64, 31.60, 27.64. Melting point: decomposition occurred at 230 °C. Elemental analysis calcd for C<sub>22</sub>H<sub>23</sub>NO<sub>4</sub> (found): C 72.31 (72.03), H 6.34 (6.34), N 3.83 (4.08). HRMS calcd for [M+H] 366.1700, found 366.1696.

## II. Peptide Characterization Tables

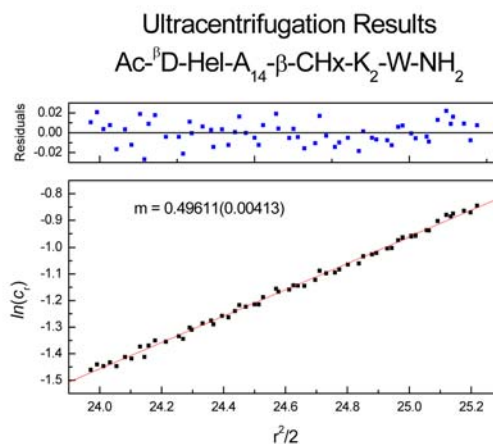
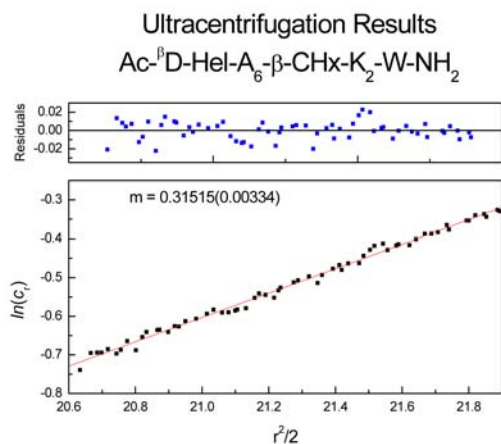
Peptide	Electrospray Mass Spectrometry (M+zH)/z Found (Expected)
Ac-W-K <sub>5</sub> -Inp <sub>2</sub> - <sup>t</sup> L- <sup>β</sup> D-Hel-β- <sup>t</sup> L-Inp <sub>2</sub> -K <sub>5</sub> -NH <sub>2</sub>	1318.84 (1320.30); 880.62 (879.56); 660.79 (659.92); 528.89 (528.14); 441.20 (440.28)
Ac-W-K <sub>5</sub> -Inp <sub>2</sub> - <sup>t</sup> L- <sup>β</sup> D-Hel-A <sub>4</sub> -β- <sup>t</sup> L-Inp <sub>2</sub> -K <sub>5</sub> -NH <sub>2</sub>	975.44 (974.28); 731.90 (730.96); 585.75 (584.97); 488.36 (487.64)
Ac-W-K <sub>5</sub> -Inp <sub>2</sub> - <sup>t</sup> L- <sup>β</sup> D-Hel-A <sub>5</sub> -β- <sup>t</sup> L-Inp <sub>2</sub> -K <sub>5</sub> -NH <sub>2</sub>	999.02 (997.95); 749.58 (748.72); 599.99 (599.18); 500.15 (499.48)
Ac-W-K <sub>5</sub> -Inp <sub>2</sub> - <sup>t</sup> L- <sup>β</sup> D-Hel-A <sub>6</sub> -β- <sup>t</sup> L-Inp <sub>2</sub> -K <sub>5</sub> -NH <sub>2</sub>	1022.72 (1021.63); 767.39 (766.48); 614.12 (613.38); 512.06 (511.32); 439.11 (438.42)
Ac-W-K <sub>5</sub> -Inp <sub>2</sub> - <sup>t</sup> L- <sup>β</sup> D-Hel-A <sub>7</sub> -β- <sup>t</sup> L-Inp <sub>2</sub> -K <sub>5</sub> -NH <sub>2</sub>	1046.42 (1045.31); 785.20 (784.24); 628.36 (627.59); 523.85 (523.16)
Ac-W-K <sub>5</sub> -Inp <sub>2</sub> - <sup>t</sup> L- <sup>β</sup> D-Hel-A <sub>8</sub> -β- <sup>t</sup> L-Inp <sub>2</sub> -K <sub>5</sub> -NH <sub>2</sub>	1070.00 (1068.99); 802.64 (802.00); 642.49 (641.80); 535.64 (535.00); 459.25 (458.72)
Ac-W-K <sub>5</sub> -Inp <sub>2</sub> - <sup>t</sup> L- <sup>β</sup> D-Hel-A <sub>9</sub> -β- <sup>t</sup> L-Inp <sub>2</sub> -K <sub>5</sub> -NH <sub>2</sub>	1093.83 (1092.67); 820.57 (819.75); 656.86 (656.01); 547.55 (546.84); 469.44 (468.86)
Ac-W-K <sub>5</sub> -Inp <sub>2</sub> - <sup>t</sup> L- <sup>β</sup> D-Hel-A <sub>10</sub> -β- <sup>t</sup> L-Inp <sub>2</sub> -K <sub>5</sub> -NH <sub>2</sub>	1117.53 (1116.35); 838.38 (837.51); 671.10 (670.21); 559.47 (558.68); 479.64 (479.01); 419.51 (419.26)
Ac-W-K <sub>5</sub> -Inp <sub>2</sub> - <sup>t</sup> L- <sup>β</sup> D-Hel-A <sub>11</sub> -β- <sup>t</sup> L-Inp <sub>2</sub> -K <sub>5</sub> -NH <sub>2</sub>	1141.24 (1140.03); 856.31 (855.27); 685.35 (684.42); 571.26 (570.52); 489.83 (489.16); 428.79 (428.14)
Ac-W-K <sub>5</sub> -Inp <sub>2</sub> - <sup>t</sup> L- <sup>β</sup> D-Hel-A <sub>12</sub> -β- <sup>t</sup> L-Inp <sub>2</sub> -K <sub>5</sub> -NH <sub>2</sub>	1164.94 (1163.71); 874.12 (873.03); 699.47 (698.63); 583.17 (583.36); 500.02 (499.31); 437.64 (437.02)
Ac-W-K <sub>5</sub> -Inp <sub>2</sub> - <sup>t</sup> L- <sup>β</sup> D-Hel-A <sub>14</sub> -β- <sup>t</sup> L-Inp <sub>2</sub> -K <sub>5</sub> -	1212.47 (1211.07); 909.61 (908.55); 727.97

NH <sub>2</sub>	(727.04); 606.87 (606.04); 520.29 (519.60); 455.44 (454.78)
Ac-W-K <sub>5</sub> -Inp <sub>2</sub> - <sup>t</sup> L- <sup>β</sup> D-Hel-A <sub>16</sub> -β- <sup>t</sup> L-Inp <sub>2</sub> -K <sub>5</sub> -NH <sub>2</sub>	1259.87 (1258.42); 945.10 (944.07); 756.34 (755.46); 630.58 (629.72); 540.68 (539.90); 473.25 (472.54)
Ac-W-K <sub>5</sub> -Inp <sub>2</sub> - <sup>t</sup> L- <sup>β</sup> D-Hel-A <sub>18</sub> -β- <sup>t</sup> L-Inp <sub>2</sub> -K <sub>5</sub> -NH <sub>2</sub>	1307.40 (1305.78); 980.84 (979.59); 784.83 (783.87); 654.28 (653.39); 560.94 (560.20); 491.06 (490.30)
Ac-W-K <sub>5</sub> -Inp <sub>2</sub> - <sup>t</sup> L- <sup>β</sup> D-Hel-A <sub>20</sub> -β- <sup>t</sup> L-Inp <sub>2</sub> -K <sub>5</sub> -NH <sub>2</sub>	1354.56 (1353.14); 1016.21 (1015.11); 813.20 (812.29); 677.86 (677.07); 581.20 (580.49); 508.74 (508.06)
Ac-W-K <sub>5</sub> -Inp <sub>2</sub> - <sup>t</sup> L- <sup>β</sup> D-Hel-A <sub>22</sub> -β- <sup>t</sup> L-Inp <sub>2</sub> -K <sub>5</sub> -NH <sub>2</sub>	1401.97 (1400.50); 1051.83 (1050.63); 841.69 (840.70); 701.56 (700.75); 601.47 (600.79); 526.55 (525.82)
Ac-W-K <sub>5</sub> -Inp <sub>2</sub> - <sup>t</sup> L- <sup>β</sup> D-Hel-A <sub>24</sub> -β- <sup>t</sup> L-Inp <sub>2</sub> -K <sub>5</sub> -NH <sub>2</sub>	1449.50 (1447.86); 1087.44 (1086.14); 870.19 (869.12); 725.39 (724.43); 621.86 (621.09); 544.36 (543.58)

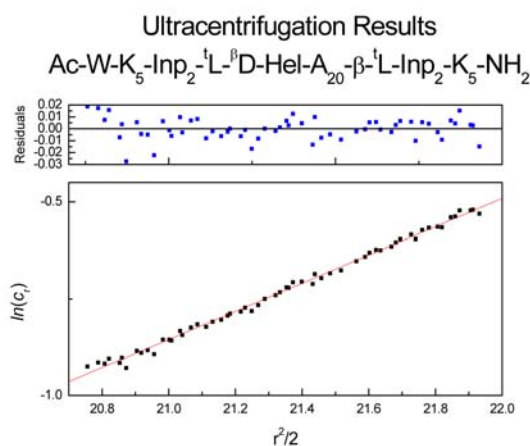
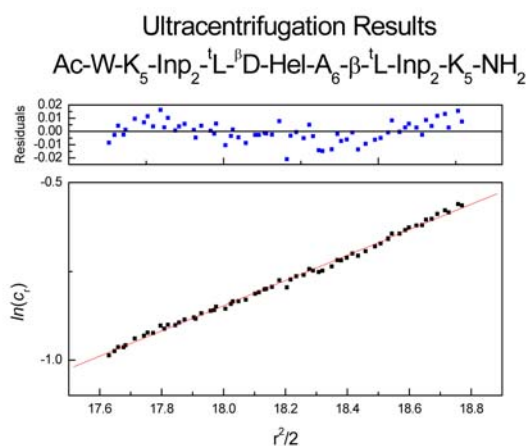
Peptide	Electrospray Mass Spectrometry (M+zH)/z Found (Expected)
Ac- <sup>β</sup> D-Hel-β-Acc-K <sub>2</sub> -W-NH <sub>2</sub>	1066.98 (1066.55), 534.09 (533.78), 356.38 (356.19)
Ac- <sup>β</sup> D-Hel-A <sub>4</sub> -β-Acc-K <sub>2</sub> -W-NH <sub>2</sub>	675.95 (675.85); 451.01 (450.90)
Ac- <sup>β</sup> D-Hel-A <sub>6</sub> -β-Acc-K <sub>2</sub> -W-NH <sub>2</sub>	747.06 (746.89); 497.87 (498.26)
Ac- <sup>β</sup> D-Hel-A <sub>8</sub> -β-Acc-K <sub>2</sub> -W-NH <sub>2</sub>	818.28 (817.93); 545.76 (543.60)
Ac- <sup>β</sup> D-Hel-A <sub>10</sub> -β-Acc-K <sub>2</sub> -W-NH <sub>2</sub>	889.02 (888.96); 593.41 (592.98)
Ac- <sup>β</sup> D-Hel-A <sub>12</sub> -β-Acc-K <sub>2</sub> -W-NH <sub>2</sub>	960.87 (960.00); 640.57 (640.34)
Ac- <sup>β</sup> D-Hel-A <sub>14</sub> -β-Acc-K <sub>2</sub> -W-NH <sub>2</sub>	1031.07 (1031.04); 687.91 (687.69)
Ac- <sup>β</sup> D-Hel-A <sub>16</sub> -β-Acc-K <sub>2</sub> -W-NH <sub>2</sub>	1102.97 (1102.07); 735.75 (735.05); 552.15 (551.54)

Peptide	Electrospray Mass Spectrometry (M+zH)/z Found (Expected)
Ac(D <sub>3</sub> )- <sup>β</sup> D-Hel-A <sub>8</sub> (2,3,3,3,-D <sub>4</sub> )-β-NH <sub>2</sub>	1102.72 (1102.71), 552.02 (551.86)
Ac- <sup>β</sup> D-Hel-A <sub>8</sub> (U- <sup>13</sup> C <sub>3</sub> , <sup>15</sup> N)-β-Acc-K <sub>2</sub> -W-NH <sub>2</sub>	804.00 (833.95), 556.44 (556.31)
Ac- <sup>β</sup> D-Hel-A <sub>6</sub> -A <sub>6</sub> (U- <sup>13</sup> C <sub>3</sub> , <sup>15</sup> N)-β-Acc-K <sub>2</sub> -W-NH <sub>2</sub>	971.88 (972.02); 647.96 (648.35)
Ac- <sup>β</sup> D-Hel-A <sub>6</sub> (U- <sup>13</sup> C <sub>3</sub> , <sup>15</sup> N)-A <sub>6</sub> -β-Acc-K <sub>2</sub> -W-NH <sub>2</sub>	971.88 (972.02); 648.21 (648.35)

### III. Analytical Ultracentrifugation Data



Sedimentation equilibrium analysis at 45,000 rpm for Ac- $\beta$ D-Hel-A<sub>n</sub>- $\beta$ -CHx-K<sub>2</sub>-W-NH<sub>2</sub> in 20 mM NaH<sub>2</sub>PO<sub>4</sub> at 2 °C (n = 6, 14).



Sedimentation equilibrium analysis at 45,000 rpm for Ac-W-K<sub>5</sub>-Inp<sub>2</sub>-<sup>t</sup>L- $\beta$ D-Hel-A<sub>n</sub>- $\beta$ -<sup>t</sup>L-Inp<sub>2</sub>-K<sub>5</sub>-NH<sub>2</sub> in 20 mM NaH<sub>2</sub>PO<sub>4</sub> at 2 °C (n = 6, 20).